

Postdiction of the Flexural Shear Capacity of a Deep Beam Without Stirrups Using NLFEM

Yang, Yuguang; de Boer, Ane; den Uijl, Joop

DOI

[10.1080/10168664.2021.1894631](https://doi.org/10.1080/10168664.2021.1894631)

Publication date

2021

Document Version

Accepted author manuscript

Published in

Structural Engineering International

Citation (APA)

Yang, Y., de Boer, A., & den Uijl, J. (2021). Postdiction of the Flexural Shear Capacity of a Deep Beam Without Stirrups Using NLFEM. *Structural Engineering International*, 31(2), 208-215.
<https://doi.org/10.1080/10168664.2021.1894631>

Important note

To cite this publication, please use the final published version (if applicable).
Please check the document version above.

Copyright

Other than for strictly personal use, it is not permitted to download, forward or distribute the text or part of it, without the consent of the author(s) and/or copyright holder(s), unless the work is under an open content license such as Creative Commons.

Takedown policy

Please contact us and provide details if you believe this document breaches copyrights.
We will remove access to the work immediately and investigate your claim.



Scientific Paper

Submitted date: [Click here to enter Date.](#)

Postdiction of the flexural shear capacity of a deep beam without stirrups using NLFEM

Yuguang Yang¹, Ane de Boer², Joop den Uijl³

¹ Delft University of Technology, Delft, the Netherlands

² Ane de Boer Consultancy, Arnhem, the Netherlands

³ Delft University of Technology, Delft, the Netherlands

Abstract

A recent contest of shear tests modelling was carried out in 2019. Teams from universities and consultancies around Europe were invited to predict the shear capacity of two reinforced concrete beams. The basics of the numerical models should be setup according the Dutch NLFEM Guideline RTD 1016-1:2017. In the contest, two reinforced concrete beams without stirrups but with a large depth (1200 mm) tested at Delft University of Technology were selected as modelling target. Most participants of the contest did not get good agreement with the test results. This paper presents a postdiction study on one of the two tests: H123. Based on this study, some adaptations are made to the recommendations of RTD 1016-1:2017 in order to better approach the test results. The intention of this contribution is to improve the existing NLFEA Guideline for practical engineering structures with uncommon reinforcement layout.

Keywords: reinforced concrete, shear failure, deep beam, without shear reinforcement, NLFEA

Introduction

Application of smeared cracking approach based Non-Linear Finite Element Method (NLFEM) is becoming more accepted in the engineering practice to model the nonlinear behaviour of structural concrete with complex loading conditions and geometries. Nowadays, general design provisions for structural concrete members such as Eurocode (CEN, 2005) and Model Code 2010 (fib, 2012) specify that the resistance of structural concrete members can be evaluated using NLFEM when simplified analytical approach may not provide an estimation with sufficient accuracy. However, modelling with NLFEM was shown to be sensitive to the choices of the modelling techniques and parameters (Belletti, et al., 2010). And it becomes time consuming if one needs many trials to get a reliable simulation. With the intension of simplifying the modelling process for engineering application, the Dutch Ministry of Infrastructure and Water Management (Rijkswaterstaat) provided a Guideline for Nonlinear Finite Element Analysis of Concrete Structures RTD 1016-1:2017 (Rijkswaterstaat, 2017a), which deals with the modelling of concrete structures using smeared cracking based NLFEM. The intension of the guideline is provide a simple general modelling approach, which will yield reliable and conservative predictions without significantly losing accuracy compared to more tailored NLFEM models.

To gain experience and build up confidence on RTD 1016-1, several validation studies on well documented experiments have been published in RTD1016-2, 3A, 3B, 3C (Rijkswaterstaat, 2017b), covering three types of structures, namely reinforced concrete beams, prestressed beams and slabs. In addition to that, two international contests based on unpublished experiments have been organized by the User Association of DIANA (Ensink, et al., 2015; Yang, et al., 2021b). The participants are from research institutes and engineering companies who use NLFEM and are familiar with RTD 1016-1. Its recent edition, in 2019, aimed at the simulation of two shear tests on reinforced concrete beams without shear reinforcement carried out at Delft University of Technology. The specimens were selected from a large research program on shear behaviour of

RC slab strips (Yang, et al., 2021b). The original goal of the research program was to investigate the size effect on the shear capacity of existing RC slab bridges without shear reinforcement.

In the contest, two unpublished shear tests on RC beams (slab strips) with 1200 mm depth were selected. The participants were asked to predict the shear capacity of these beams with any approach including numerical and analytical models. When NLFEM would be applied, it was advised to follow RTD 1016-1 (but this was not compulsory). The provided information before the competition included the detailed geometry of the specimen, the reinforcement configurations, the test setup and the mechanical properties of concrete and reinforcement (also listed in Table 1). The results of the simulations were disappointing, despite that most contributions followed the aforementioned design codes and guidelines. On average, an overestimation of more than 140 % of the experimental capacity was obtained from the total 10 contributions submitted to the contest. A summary of the contest and the results was reported in (Yang, et al., 2021b; Yang, et al., 2021b). To the owners of existing large infrastructural structures, like Rijkswaterstaat, the contest results might raise the following question:

Is RTD 1016-1 still reliable, and how should RTD 1016-1 be improved with the obtained information?

Out of the two beams in the contest: H123 ($\rho_l = 1.14\%$) and H352 ($\rho_l = 0.36\%$), H123 was selected in the present study considering that it had a more practical longitudinal reinforcement ratio. With the test results known, this paper focuses on searching for an improved set of choices based on a postdiction study. As for NLFEM, in addition to the loading conditions and the material properties, the choices of modelling parameters and solution strategies may affect the simulation results as well. The intention of the present study is to investigate the possibility of approaching the test results by adjusting these parameters and demonstrate a step-by-step approach of improving the modelling flexural shear failure of deep RC members without shear reinforcement. The study is mainly based on the commercially available NLFEM software package DIANA, to avoid bias another software package ATENA is used in an additional validation case.

Shear test on beam H123

The shear test H123 was designed to investigate the size effect of a realistic configured RC member without shear reinforcement. The dimensions and the reinforcement configurations of the test specimen are given in Figure 1. As shown, the specimen was loaded by a single point load at mid-span, with the left side being considered as test span. Half of the longitudinal reinforcement bars were bent up to the top side of the specimen with the other half welded at the bar ends to the bent-up bars, in order to ensure sufficient anchorage at the beam ends. The reinforcement bars were arranged in two layers, however no spacing was specified between the two layers, which were connected to each other by pit welding at a few spots.

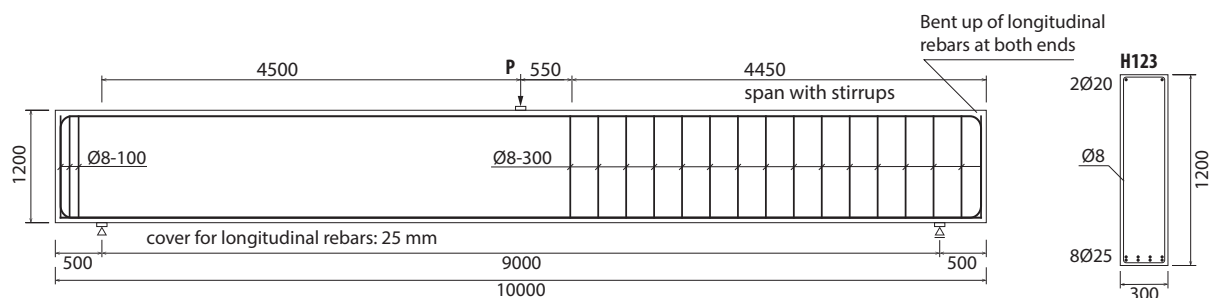


Figure 1. Dimensions, test conditions and reinforcement configurations of H123.

At the date of the experiment, several material properties were tested in the lab using concrete cubes of 150 mm. The average values of these properties, which were given to the participants of the contest, are shown in Table 1. In the contest, it depended on the users' interpretation for the input in their NLFEM simulations based on this information.



Table 1. Material parameters obtained from lab tests.

Parameter		value	units
Concrete strength (from 150 mm cube tests)	$f_{c,cube}$	86.9	MPa
Concrete tensile strength (from splitting tests of 150 mm cubes)	$f_{ct,split}$	5.7	MPa
Maximum aggregate size	d_a	16	mm
Density of concrete	ρ_c	23.9	kN/m ³
Yield stress reinforcement	f_{yk}	583.9	MPa
Ultimate stress reinforcement	f_{tk}	683.9	MPa

In the test, the beam failed at a maximum load of 445 kN. The crack patterns of the specimen at $P = 400$ kN and after the formation of the flexural shear crack are shown in Figure 2. As indicated by the crack pattern at 400 kN and 445 kN, the critical shear crack initiated from the last flexural crack. Further propagation of the flexural shear crack resulted in failure of the specimen. The observed crack pattern is utilized for comparison with the output of the simulation results.

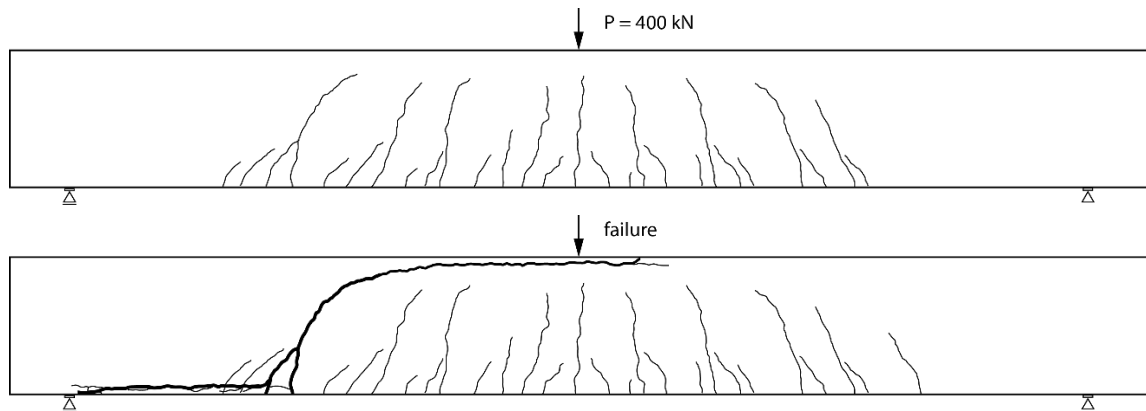


Figure 2. Crack pattern of H123 at the last load level before failure (top figure) and the crack pattern after failure (bottom figure).

In the test, the critical shear crack formed from the already present flexural crack at 400 kN. At the peak load, two secondary cracks developed from one of the major flexural cracks into the compression zone and along the longitudinal reinforcement. The propagation process of these two branches was very unstable, which leads to the sudden drop of the bearing capacity and the increase of the deflection. This type of failure is typically defined as flexural shear failure as suggested by (Yang, 2014). The unstable propagation of the flexural shear crack at failure leads to a drastic change of the deformation and stress distribution in the whole beam. This is usually difficult to be captured by numerical models without lack of convergency.

Modelling choices based on the RTD 1016-1 guideline

In addition to the information provided by the call of the contest (shown in Table 1), the missing parameters for the NLFEM are obtained following the instructions of RTD1016-1, which leads to the additional material and analysis parameters given in Table 2.

Out of the listed parameters, this study will first discuss the choices of the concrete parameters which are not always directly reflected by lab specimen tests, such as the concrete tensile strength f_{ctm} . Next, the study discusses the influences of the modelling choices and analysis parameters to the simulation results. These parameters includes: rotating/fixed crack model, element size and bond-slip model. After comparing with the

test results, further improvements of the modelling choices and analysis parameters that do not relate to the material properties are made.

Table 2. Additional material and nonlinear analysis parameters

Parameter	Value
f_{cm}	71.2 MPa
G_f	157.3 N/m
G_c	250× G_f
Poisson ratio	0.15
Crack model	rotated
f_{ctm}	4.44 MPa
Young's modulus	39.2 GPa
Convergence	Energy + Force
Element size over height girder	100 mm (Mapped mesh)
Arclength	Regula
Model of Reinforcement	Bar element
Bonded/bond slip	Perfect bond

Regarding the concrete tensile strength, in the announcement of the contest, the tensile strength of the concrete was reported to be 5.7 MPa, which was obtained by splitting tensile tests. However, the direct tensile strength f_{ctm} should be used when analysing the tensile behaviour of concrete in a NLFEM. This is also recommended by RTD1016-1 and other design codes such as the *fib* Model Code 2010. In this study the concrete tensile strength f_{ctm} is directly derived from the concrete compressive strength.

The validation studies reported by (Rijkswaterstaat, 2017c), suggest to apply the total strain rotating crack model as the default choice of the material model. As demonstrated by (Rots, 1989), the rotating crack model turns out to be more robust against shear locking, thus it typically provides a lower prediction than the fixed crack model type. For engineering practice, the ease of use of the rotating crack model combined with its conservative prediction is considered as great benefit. Thus in RTD 1016-1 rotating crack model is suggested. However, as suggested in (Yang, et al., 2017) the shear capacity of RC members without shear reinforcement may be affected by the crack pattern, while rotating crack model is known not to be able to accurately simulate the crack pattern. In the study, both the rotating crack model and the fixed crack model are therefore employed. Following the default settings of the software, the rotating crack model is typically used in DIANA and the fixed crack model in ATENA.

In terms of element size, mesh sensitivity study is generally recommended by most NLFEM packages (DIANA FEA, 2020; Cervenka & Jendele, 2009) as well as design codes (fib, 2012). Although with the introduction of the crack band theory proposed by (Bažant & Oh, 1983), the effect of element size on the cracking behaviour of concrete is taken into account for models with regular mesh layout. For shear simulations, recent studies reported by (Slobbe, et al., 2013) and (Cervenka, et al., 2016) showed that the element size and orientation still have a clear influence on the prediction results. Therefore, the influence of element size is chosen as a modelling parameter to be studied in this paper. RTD 1016-1 suggests a maximum element size of $h/6$ over the height of the beam. It is expected that a smaller element size will lead to more accurate prediction. Thus to simulate the H123 beam with a height of 1200 mm, a larger number of elements (more than 6 elements) over the height of the beam is foreseen. In (Červenka, et al., 2018), the maximum element size for members with tensile cracking is suggested to be the expected crack spacing. The minimum element size was not introduced yet in RTD 1016-1 in 2017. In (Bažant, et al., 1984; Červenka, et al., 2018) the minimum element size was suggested to be 1.5 – 3 times the maximum aggregate size in order to fulfil the basic assumption of local continuum theory.



The third study parameter is the bond-slip model of the reinforcement bars. In RTD 1016-1, a reinforcing bar is modelled by embedded elements with perfect bond to concrete. It means that when the tensile strain of the reinforcement becomes larger than the cracking strain of concrete, the concrete elements crack in order to fulfil the kinematics conditions. The introduction of a bond-slip model when modelling the embedded reinforcement leads to a more realistic crack pattern at the level of the tensile reinforcement. This is considered as an option to provide a more accurate prediction to model failure modes which are sensitive to the crack propagation like the H123 beam. In this study the bond-slip model proposed by (Shima, et al., 1987) is selected in the reference model. The model describes the interaction between a reinforcing bar and the surrounding concrete at macro level. In this model reduction of bond stress due to local failure of the interface is not considered. Thus it needs only an input value for the compression strength. The bond-slip model of Shima is adapted in some of the DIANA models. The bond-slip model of the MC2010 (fib, 2012), on the other hand, takes into account different bond failure modes (pull-out and splitting), which results in different bond stress-slip relations. With the bond-slip model suggested by Model Code 2010, the unloading of the bond stress due to local failure under large slip can be modelled as well. The Model Code 2010 bond-slip model is adapted in the ATENA model (Jendele & Cervenka, 2006) presented in this study.

Beside the modelling choices of the simulation, the convergence criteria may affect the results as well. They may be chosen amongst displacement, force or energy based criteria, coupling two or all three criteria. For each choice, the values for the tolerance of the criteria will affect the simulation results. A recent study reported in (de Putter, 2020) shows this effect. In the study, it was recommended that for simulations with brittle failures like the flexural shear failure of RC members without shear reinforcement, in order to continue the simulation with reasonable accuracy, it is not necessary to continue simulation steps with all the criteria fulfilled. In RTD 1016-1, using the maximum values of 0.001 for the energy criterion and 0.01 for the force criterion is recommended. Imposing multiple convergence criteria in a simulation often leads to unnecessary load steps or even early divergence in critical load step(s). In engineering practice, in order to go over such critical load step(s), a choice of relaxing the convergence criteria or reducing the number of criteria is employed. In this paper, with the intention of simplifying the study, only the Energy norm (criterion) amongst the other criteria is selected to study further, to be in line with RTD 1016-1.

In test H123A, the load was applied by an actuator using displacement control due to safety considerations. However, most structures in engineering practice are designed for force controlled loads such as gravity, wind pressure or traffic loading. Ideally NLFEM simulations loaded by either displacement or force control should give comparable results. Taking that into account, in this study both loading methods are applied to the same model in order to evaluate the potential difference between the two loading approaches. They are distinguished by a (displacement control) or b (force control) after the simulation No. when they are referred in the text.

Effect of element size

The effect of element size in the simulation is studied first in three simulations using element sizes varying from 200 mm to 50 mm, which leads to 6 to 24 elements in the height of the beam. The configurations of Simulations 01 – 03 are listed in Table 3. The basic modelling choices follow RTD 1016-1 and Table 2. The convergence limit of Energy is set to 1.0E-4. According to RTD 1016-1, all load steps should converge till the ULS is reached with a convergence value for Energy tolerance of 1.0E-3.

Table 3. Results of element size simulations

Simulation No.	Element size [mm]	$P_{max,disp}^{1)}$ [kN]	$P_{max,disp}/P_{Test}$ [-]	$P_{max,forc}^{2)}$ [kN]	$P_{max,disp}/P_{Test}$ [-]	$P_{max,forc}/P_{max,disp}$ [-]
D01	200	432	0.97	441	0.99	1.02
D02	100	365	0.82	346	0.77	0.95
D03	50	301	0.68	279	0.63	0.93

- 1) $P_{max,disp}$ is the maximum applied load before the convergence criterion was reached. In the simulation, the load was applied by displacement control. Accordingly, the simulations are named as D01a – D03a.

- 2) $P_{max,forc}$ is the maximum applied load before the convergence criterion was reached. In the simulation, the load was applied by force control. Accordingly, the simulations are named as D01b – D03b.

Table 3 shows the results of the three simulations with different element sizes. The maximum load level of Simulation D01a is close to the experimental load level. Using a finer mesh results in a reduction of the ultimate load till a maximum load of 279 kN from D03b. Both smaller element models show a lower ultimate load with force controlled (b series models) than with displacement controlled loading (a series models). However the difference between both loading methods is rather small, at most 7.3%. Figure 3 shows the crack patterns of Simulation D02 using both displacement control and force control analyses.

The results of the simulation indeed demonstrates the influence of element size upon the failure load. However this conclusion is rather different from what was reported in (Cervenka, et al., 2016). In the study of Cervenka et.al., models with larger element size leads to lower capacity. However, our simulations using both loading methods show that by using a larger element size, higher capacity is predicted. Further study is still needed to investigate the reason of the mesh dependency in both studies and the possible solutions to resolve it.

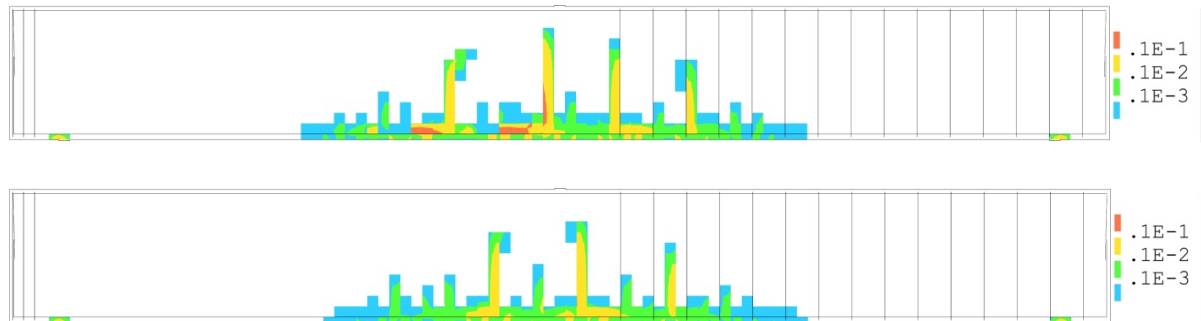


Figure 3 Crack pattern just before ULS Load level from Simulation D02a displacement controlled (top) and from Simulation D02b force controlled (bottom).

In terms of crack patterns, Figure 3 shows that the different loading methods give rather similar predictions, with slightly different magnitude of the maximum crack strains before failure. The red and yellow coloured strains show that cracks initiate along the longitudinal reinforcement. Similar cracking is reported in (de Putter, 2020). Further loading leads to the loss of load bearing capacity. As comparison, the crack pattern of H123 at the load step before failure ($P = 400$ kN) is shown in Figure 2. The crack pattern of both methods turns out to be rather comparable to the measured crack pattern, although the final crack pattern at failure cannot be shown because the critical shear crack only occurred at the very last load step which leads to divergence of the simulation. Most cracks before failure were flexural cracks, with which limited rotation of the crack is expected. Nevertheless, at several spots at the bottom of the flexural cracks, initiation of longitudinal cracks can be observed along the reinforcing bars. This observation shows that an accurate bond-slip model is needed as an additional input option to get a more realistic behaviour around the reinforcement bar in order to obtain a more accurate failure load.

Bond slip model and analysis parameters

In Simulation D01 – D03, no clear shear crack was observed before failure. This could also because of a too relaxed convergence criterion. In order to avoid the discussions about the choice of the convergence criterion, another set of simulations (Simulations D04 – D06) was developed. From Simulation D01 – D03 it was concluded that an accurate bond-slip model might be a critical requisite for the simulation. Thus, the bond-slip model of Shima (Shima, et al., 1987) is also introduced in the new set of simulations. The FE models have a mesh with element size of 50 mm. This choice is based on the assumption that models with finer mesh size are able to represent the behaviour of a structure in more detail, thus has the potential to provide better accuracy. The main difference between the three simulations is the value of the energy norm. In Simulation D04, the energy norm is set to 1.0E-3 as suggested by RTD 1016-1, while the other two simulations employ an energy norm of 10.E-4 and 10.E-5, respectively, see Table 4. Both the displacement control and force control method are used in these simulations.



Table 4. Results of analyses on convergence energy criterion, all simulations use element size of 50 mm.

Simulation No.	Energy norm	Arc length control	$P_{max,disp}$ [kN]	$P_{max,disp}/P_{Test}$ [-]	$P_{max,forc}$ [kN]	$P_{max,forc}/P_{Test}$ [-]	$P_{max,forc}/P_{max,disp}$ [-]
D04	1.0E-3	Automatic	392.3	0.88	348.5	0.78	0.89
D05	1.0E-4	Automatic	348.7	0.78	372.5	0.84	1.07
D06	1.0E-5	Automatic	378.2	0.85	364.4	0.82	0.96
D07	1.0E-4	Manual	-	-	456.9	1.03	-
D08	1.0E-5	Manual	-	-	405.9	0.91	-

Table 4 shows the results of the second series of simulations. Comparison of the results with the 50 mm element size simulation in table 3 and the results of table 4 yields the first conclusion that the ultimate load level is increased by implementing the bond-slip model. A second conclusion is that the load level does not change significantly when the tolerance value is increased. Both loading methods show this aspect. The difference between model predictions and test results is around 20%. Although more simulations are still needed to draw solid conclusions, one may consider that introduction of a bond-slip model may change the results of the simulations, and could provide a more reasonable estimation.

The crack pattern of Simulation D05 is shown in Figure 4. Compared to Figure 3, a more developed pattern of cracks is present by the introduction of the bond-slip model. Also the crack spacing at mid-depth of the beams turns out to be more representative to that observed in the experiments in Figure 2. Compared to the perfect bond model, a realistic bond-slip model enables the localization of crack opening amongst the elements at the rebar level, that clearly results in a more realistic crack pattern. Thus this can be seen as an improved result.

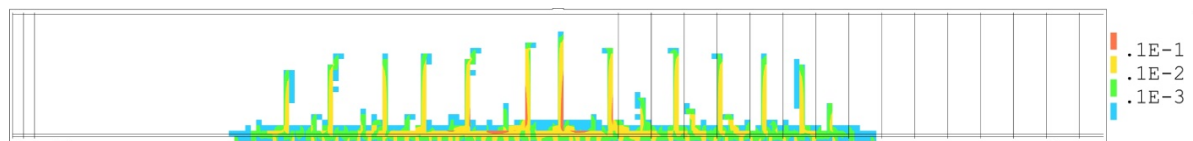


Figure 4. Overview crack pattern force controlled method for Simulation D05.

The ratio between the maximum load observed in the experiments (445 kN) and the simulations (348 – 392 kN) is still low. A further improvement was made by adjusting the arc length analysis. As suggested by (Verhoosel, et al., 2008), the adaption of arc length analysis may improve the stability of the analysis, thus being able to obtain the snap-back behaviour of the structure. RTD 1016-1 recommends arc length analysis to improve the convergence of the simulation. As an additional improvement, the default automatic arc length approach is replaced. In the new simulations, the control displacement is set to the bottom fibre of the left half length of the girder. Thus, the crack length of the bottom fibre of the concrete becomes more important in determining the load factor in the arc length calculation. Two new simulations are made in the additional study, Simulation D07 and D08 in table 4. Since from the previous study, the different loading approaches show very limited influence to the simulation results, in Simulation D07 – D08 only force control was applied. When comparing with the test results, the simulated ultimate load reached 90% of the experimental result and on the lower side. Hence, the adjustment of the arc length approach can be considered as a further improvement.

As was done in (Belletti, et al., 2010) and (Rijkswaterstaat, 2017b), test H123 is also simulated with the software package ATENA. Being different from the models in DIANA, the rebars in ATENA are modelled using embedded elements, but incorporated explicitly with a bond-slip model. The bond-slip model proposed in the Model Code 2010 (fib, 2012) is employed. The bond-slip model suggested in Model Code 2010 includes the softening parts of bond-slip relationship. And it can consider different bond failure modes. The model is numbered as Simulation A01 in this paper. The ultimate load level of Simulation A01 is 479 kN, which is similar to the simulation with the Shima bond-slip model and – more important – still a reasonable estimation. The corresponding crack pattern is given in figure 5. As a standard approach in ATENA, a fixed smeared crack

model with a crack width based shear retention factor is used in the simulation. Besides, when the predefined convergence criterion is not reached within 50 iterations, the program accept a relaxed convergence criterion. The crack patterns of the specimen before and after the peak load are indicated in Figure 5. With the fixed crack model, the crack pattern does not change with the change of the principal stress direction, thus a realistic flexural shear crack can be simulated as shown in Figure 5. In addition, in Simulation A01, it is possible to reach the descending branch of the load – deflection relations, see figure 6. That provides additional confidence of the simulations provided by DIANA, in which further loading were not possible. The crack pattern given by the simulations of ATENA compares well with the crack pattern after failure in figure 2. In ATENA, a realistic crack pattern is also found with a reference model with perfect bond. The simulation is not demonstrated in the paper.

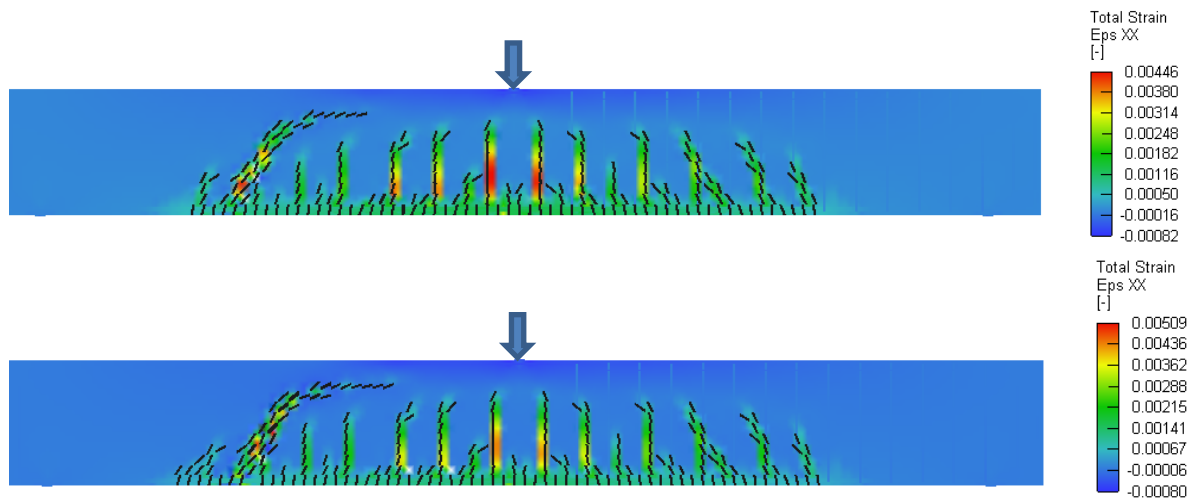


Figure 5. Crack pattern (crack width > 0.01 mm) and horizontal strains in ATENA simulation (Simulation A01) with MC2010 bond splitting model at ULS load level (top, 479 kN) and just after maximum load (bottom) (2D-model with 100x100 mm quadratic elements, displacement control, Arc Length solution method).

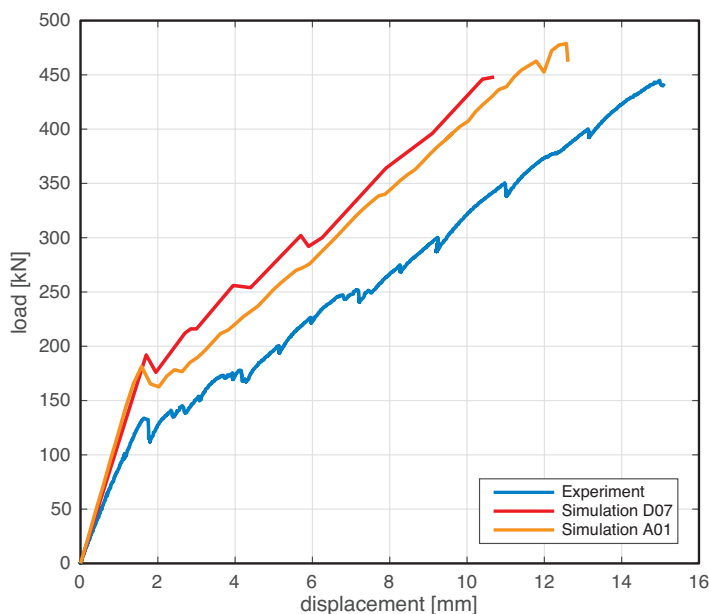


Figure 6. Load displacement diagrams of Simulation D07 with Shima bond slip model using DIANA and Simulation A01 with MC2010 A01 bond-slip model using ATENA.

Based on the discussion above, Simulation D07 and Simulation A01 are chosen as the final representative models. Figure 6 shows the load-displacement diagram of both models and that from the experiment. The displacement shown in the figure is the maximum deflection under the loading point. The comparison shows that both Simulation D07 and A01 provide rather similar load-deflection relationship, and they compare well



with the experimental observation. The main difference lies in the stiffness, which can be attributed the long term deformation of concrete during the loading process. Comparing the stiffness of the first branches in Figure 6 shows a reduction with a factor 0.74 from simulation to the test (Yang, et al., 2021b) and 0.77 in the second branches. In an experiment that takes several hours a certain amount of creep will occur, which can be simulated with a lower elastic modulus. Similar observation has been reported in (Cervenka, et al., 2016). Besides, the first cracking loads in the simulations are higher than that observed in the experiments. This could partly relate to the same phenomenon. Under sustained loading a reduced tensile strength may be expected with comparable deformation as suggested by (Rusch, 1960; Reinhardt & Cornelissen, 1985). In addition, the variation in concrete strength may result in a lower fracturing load (Tran & Graubner, 2018).

Discussions and recommendations

In this study, the following steps are made to improve the simulation, which can be summarized as advices for the engineering practice when dealing with similar simulations:

1. Evaluation of mesh dependency.
2. Introduction of a bond-slip model when crack propagation at the level of the longitudinal reinforcement is critical to the failure.
3. Further refinement of solving strategy (for example, manual selection of control displacement in an arc length analysis).
4. For better crack pattern adaption of fixed crack model.

In this paper it is shown that indeed the influence of the so called modelling choices that were previously considered to be less important may affect the simulation results considerably in this special situation. It shows the risk of using NLFEM when it is applied on modelling of structure members with large dimensions and brittle failure mode. In addition to that, the proposed improvement steps, have shown to give a realistic approach to further improvement of the simulations. With this approach, simulations with good agreement to the experimental results can be obtained. Despite that, as the intension of the paper is not to provide a systematic study on how to accurately perform non-linear simulation of the flexural shear behaviour of RC beams, further studies on the effect of the following aspects remain open:

1. The effect of element size to the simulation of structural members with large dimensions.
As discussed earlier, the presented study shows a clear influence of element size on the simulation results. However, an opposite conclusion from that reported in a previous study (Cervenka, et al., 2016) was obtained. To get a clear picture on the influence of element size in shear simulations, further study is still necessary.
2. The effect of the bond-slip model in the simulation.
In this study, better results were reported after the introduction of a bond-slip model. Further validation is needed on the choice of bond-slip model and the robustness of the simulation when such bond-slip model is introduced.
3. In the simulations, a dowel crack along the longitudinal reinforcement was often observed during the propagation of the critical shear crack. As the embedded reinforcement is usually considered as bar elements, the bending stiffness, which is considered as the reason of dowel cracking, cannot be simulated with this element type. Introduction of a beam type reinforcement element may further improve the simulation.

Conclusions

This paper presents a post-diction study on the shear failure of specimen H123, with the intention to provide a simple stepwise approach to improve simulations including flexural shear failure. It is demonstrated that the simulation of the experimental results of H123 can be improved by refining modelling choices. The study provides a practical stepwise example starting with a basic model, proposed by RTD 1016-1. The following conclusions can be drawn:

1. The influence of the element size on the model simulation turns out to be rather complicated. This study yields a different conclusion than the earlier study reported by (Cervenka, et al., 2016). Further study on this topic is still needed.

2. Both the total strain rotating crack model and the total strain fixed crack model may provide sufficient accuracy. However, the fixed crack model is able to provide a more realistic crack pattern.
3. For the simulation of the shear behaviour of RC members without stirrups, introduction of a bond-slip model may improve the simulation results. Within this study both the bond-slip model suggested in Model Code 2010 and the model proposed by Shima give predictions closer to the test results than simulations with perfect bond.
4. More beams without stirrups should be simulated to quantify the model uncertainty for NLFEM simulation on the shear behaviour of RC members.
5. The work presented in the paper can be interpreted as a warning for users of RTD 1016-1 in case of deep beams without shear reinforcement. The simulation of such type of structures turns out to be more sensitive to the choices of the modelling parameters than for other types of structures.

Acknowledgements

The authors would like to acknowledge the Dutch ministry of infrastructure and environment (Rijkswaterstaat) for financially support the experimental research program in which the test of H123 was included.

References

- Červenka, J., Červenka, V. & Laserna, S., 2018. On crack band model in finite element analysis of concrete fracture in engineering practice. *Engineering Fracture Mechanics*, Volume 197, pp. 27-47.
- Bažant, Z., Belytschko, T. & Chang, T., 1984. Continuum theory for strain-softening. *Journal of Engineering Mechanics*, 110(12).
- Bažant, Z. & Oh, B., 1983. Crack band theory for fracture of concrete. *Materials and Structures*, 16(94).
- Belletti, B., den Uijl, J., Hendriks, M. & Damoni, C., 2010. *Developing Standardized Guidelines for a Safety Assessment of Shear-Critical RC Beams Based on Nonlinear Finite Element Modeling*. Washington, s.n.
- CEN, 2005. *Eurocode 2: Design of Concrete Structures - Part 1-1 General Rules and Rules for Buildings. NEN-EN 1992-1-1*. s.l.:s.n.
- Cervenka, V., Cervenka, J., Pukl, R. & Sajdlov, T., 2016. Prediction of shear failure of large beam based on fracture mechanics. *FraMCoS-9*.
- Cervenka, V. & Jendele, L., 2009. *ATENA program documentation part 1: Theory*, Prague: Cervenka Consulting.
- de Putter, A., 2020. *Towards a uniform and optimal approach for safe NLFEA of reinforced concrete beams: Quantification of the accuracy of multiple solution strategies using a large number of samples*, Delft: s.n.
- DIANA FEA, 2020. *DIANA User's Manual (release 10.3)*, Delft: s.n.
- Ensink, S. W. H., van der Veen, C. & de Boer, A., 2015. Shear or bending? Experimental results on large t-shaped prestressed concrete beams. *Proceedings of the 16th European bridge conference*.
- fib task group 8.2, 2008. *Constitutive modelling of high strength/high performance concrete*, s.l.: fib.
- fib, 2012. *Model Code for Concrete Structures 2010*. Lausanne: Ernst & Sohn.
- Jendele, L. & Cervenka, J., 2006. Finite element modelling of reinforcement with bond. *Computers and Structures*, Volume 84, p. 1780–1791.
- Lantsoght, E., de Boer, A., van der Veen, C. & Hordijk, D., 2019. Optimizing Finite Element Models for Concrete Bridge Assessment With Proof Load Testing. *Front. Built Environ.*, p. <https://doi.org/10.3389/fbuil.2019.00099>.
- Reinhardt, H. & Cornelissen, H., 1985. Sustained tensile tests on concrete (in German); Zeitstandzugversuche an Beton. *Bauverlag Wiesbaden*, pp. 162-167.
- Rijkswaterstaat, 2017a. *Guidelines for nonlinear finite element analysis of concrete structures. RTD 1016-1*. s.l.:s.n.



450 Rijkswaterstaat, 2017b. *Validation of the Guidelines for Nonlinear Finite Element Analysis of Concrete*
451 *Structures - Part: Overview of results. RTD 1016-2*, s.l.: s.n.

452 Rijkswaterstaat, 2017c. *Validation of the guidelines for NLFEA of RC structures Part Reinforced*
453 *beams(RTD1016-3A), Prestressed beams(RTD1016-3B) and Slabs(RTD1016-3C)*, Delft: s.n.

454 Rots, J., 1989. Crack models for concrete: discrete or smeared? fixed, multi-directional or rotating?.
455 *Heron*, 34(1).

456 Rusch, H., 1960. Researches Toward a General Flexural Theory for Structural Concrete. *Journal of the*
457 *American concrete institute*, 57(1), pp. 1-26.

458 Shima, H., Chou, L.-L. & OKAMURA, H., 1987. Micro and Macro Models for Bond in Reinforced
459 Concrete. *Journal of the Faculty of Engineering*, 39(22).

460 Slobbe, A., Hendriks, M. A. & Rots, J., 2013. Systematic assessment of directional mesh bias with
461 periodic boundary conditions: applied to the crack band model. *Engineering Fracture Mechanics*,
462 Volume 109.

463 Tran, N. L. & Graubner, C.-A., 2018. Influence of material spatial variability on the shear strength of
464 concrete members without stirrups. *BETON-UND STAHLBETONBAU International Probabilistic*
465 *Workshop 2018*.

466 Verhoosel, C. V., Remmers, J. J. C. & Gutiérrez, M. A., 2008. A dissipation-based arc-length method
467 for robust simulation of brittle and ductile failure. *International journal for numerical methods in*
468 *engineering*.

469 Yang, Y., 2014. *Shear behaviour of reinforced concrete members without shear reinforcement*, Delft:
470 s.n.

471 Yang, Y., de Boer, A. & Hendriks, M., 2021b. *A contest on modelling shear behaviour of deep concrete*
472 *slab strips using non-linear FEM*. Lisbon, s.n.

473 Yang, Y., den Uijl, J. & Walraven, J., 2017. Shear Behavior of Reinforced Concrete Beams without
474 Transverse Reinforcement Based on Critical Shear Displacement. *Journal of Structural Engineering*,
475 143(1).

476 Yang, Y., Naaktgeboren, M. & van der Ham, H., 2021b. *Shear capacity of RC slab structures with low*
477 *reinforcement ratio - an experimental approach*. Lisbon, s.n.

478